Discovery of a multipotent cell type from the term human placenta

Sangeetha Vadakke-Madathil[1*], Bingyan J Wang[1], Micayla Oniskey[1], Fumiko Dekio[2], Rachel Brody[2], Shari Gelber[3], Rhoda Sperling[4] and Hina W. Chaudhry[1*]

[1]Department of Cardiology, [2]Department of Pathology, [3]Department of Obstetrics/Gynecology and Maternal-Fetal Medicine, Icahn School of Medicine at Mount Sinai, New York, NY, USA

Abstract

We report a unique population of multipotent cells isolated from the term human placenta, for the first time, that can differentiate into cardiomyocytes and vascular cells with clonal proliferative ability, migratory ability, and trancriptomic evidence of immune privilege. Caudal-type homeobox-2 (CDX2) is a conserved factor that regulates trophectoderm formation and placentation during early embryonic development but has not previously been implicated in developmentally conserved regenerative mechanisms. We had earlier reported that Cdx2 lineage cells in the mouse placenta are capable of restoring cardiac function after intravenous delivery in male mice with experimental cardiac injury (myocardial infarction). Here we demonstrate that CDX2-expressing cells are prevalent in the human chorion and are poised for cardiovascular differentiation. We examined the term placentas from 106 healthy patients and showed that isolated CDX2 cells can spontaneously differentiate into cardiomyocytes, functional vascular cells, and retain homing ability *in vitro*. Functional annotation from transcriptomics analysis supports enhanced cardiogenesis, vasculogenesis, immune modulation, and chemotaxis gene signatures in CDX2 cells. CDX2 cells can be clonally propagated in culture with retention of cardiovascular differentiation. Our data supports further use of this accessible and ethically feasible cell source in the design of therapeutic strategies for cardiovascular disease.

23 **Main**

24 The successful use of cell therapy for cardiac repair hinges on several critical attributes:
25 cells must have the capacity for cardiomyocyte differentiation akin to embryonic stem cells (ES)
26 and induced pluripotent cells (iPSC), they must exhibit clonality, possess an immune-modulatory
27 capacity for allogeneic administration, and ideally the ability to home to sites of injury. Cell
28 therapy for cardiac purposes has been demonstrated to be safe by numerous preclinical and clinical
29 studies[1-4], however; there has been a glaring lack of *bona fide* cardiac differentiation amongst cell
30 types administered in clinical trials thus far[5-7]. Despite a multitude of clinical cell therapy trials,
31 which largely sought to inject stem/progenitor cells or cardiomyocytes derived from such cells into
32 the heart, true progress in actual cardiomyocyte repopulation with a significant restoration of
33 myocardial function has remained a distinct challenge. Injection of cells even if they have
34 differentiated to nascent cardiomyocytes into the complex cardiac milieu is unnatural, and not
35 rooted in developmental pathways supporting organogenesis and tissue healing. Regenerative
36 biology must rely on exploring evolutionarily preserved healing mechanisms to maintain and
37 restore homeostasis. Gestation is one such condition that requires extensive cellular cross-talk to
38 maintain homeostasis. The human placenta is a vital organ responsible for supporting embryonic
39 development and facilitating the exchange of nutrients and waste between the mother and fetus.
40 Placenta and the fetal heart are thought to undergo concurrent evolution sharing major
41 developmental pathways[8-10]. Studies suggest that the placenta may regulate cardiac ventricular
42 wall expansion once maternal blood flow is established[11]. This implies that cells with regenerative
43 ability within the placenta may be better poised to support cardiogenesis. Our focus turned to
44 placental cells after clinical observations of patients with peripartum cardiomyopathy. This
45 etiology of heart failure enjoys the highest recovery rate (~50%) amongst all forms of heart

46 failure[12] and we postulated that progenitor cells from the fetus or placenta might be playing a role
47 in this recovery.

48 Stem or progenitor cells from the placenta are developmentally closer to embryonic stem
49 cells but functionally different and non-tumorigenic[13]. Caudal type homeobox-2 (CDX2) is a
50 conserved factor expressed that regulates trophoblast stem cell differentiation and is required for
51 proper placental development[14,15]. We had discovered a novel role of Cdx2 cells in murine
52 gestation as a preclinical model of myocardial infarction (MI) in pregnant mice elicited the specific
53 migration of fetal placental cells into the injured maternal heart to form cardiovascular cells[16].
54 Furthermore, isolated murine placental Cdx2 lineage cells formed spontaneously beating
55 cardiovascular cells *in vitro* and contributed to cardiac repair *in vivo* after intravenous infusion
56 even in male mice subjected to myocardial infarction[17].

57 In this study, we isolated CDX2-expressing cells from 106 human term placentas. For
58 research purposes, we utilized a human CDX2 promoter-driven lentivirus-based mCherry
59 fluorescence reporter. Transcriptomic analyses comparing human embryonic cells, term placental
60 CDX2 cells, and term placental non-CDX2 cells were performed to gain deeper insights into the
61 functional differences between these cell types. We further investigated the stem/progenitor
62 function and cardiovascular commitment of human placental CDX2 cells to ascertain their
63 potential as a novel therapeutic for cardiovascular disease.

64 **Results**

65 **Cells expressing CDX2 are enriched within the chorionic region of the human placenta**

66 The homeodomain protein CDX2 is involved in embryonic development and placentation. To
67 detect if CDX2 is present in human placentas, we carried out a multi-parametric approach and
68 examined the transcript expression from an earlier time point in first-trimester chorionic villus

69 samples (CVS) and later within the chorionic cells (fetal) from term healthy placentas. CDX2
70 mRNA was detected in both CVS and chorionic regions (**Fig.1a**). Sanger sequencing and analysis
71 of the output FASTA sequences further confirmed sequences specific to human CDX2 mRNA
72 (Supplemental data). Immunoblot analyses detected CDX2 protein in the term chorion (~40kDa)
73 with the conventional doublet pattern representing two isoforms from alternative splicing (**Fig.**
74 **1b**). HeLa cells showed a lower endogenous expression of CDX2, whereas DLD1 served as a
75 positive control. Immunohistochemistry revealed that CDX2 protein was enriched in the fetal
76 chorionic region of the human placenta and not in the fetal amnion (Extended Data **Fig.1a,b**).
77 CDX2 was detected in the villous region (**Fig 1c**), particularly within the cytotrophoblast layer of
78 the chorion (Extended Data Fig.1a,b). We found that most CDX2-expressing cells co-localized
79 with the trophoblast marker Cytokeratin 7 (**Fig. 1c, d**, CKT7- 95 ± 5.0%) and were associated with
80 Human Leukocyte Antigen G (**Fig. 1e, f,** HLAG- 50.5±5%), which is mostly expressed in
81 extravillous trophoblast progenitors and is critical for inducing an immune-tolerant
82 microenvironment in the placenta. This data shows that CDX2 is expressed in the term human
83 placenta and expresses pan trophoblast marker cytokeratin 7 and extravillous marker HLA-G.

84 **Clonality, *in vitro* expansion, and homing potential of CDX2 cells**

85 The initial isolation of viable cells expressing CDX2 was challenging because no surface
86 markers had been identified for enrichment thus far. In this study, we developed a CDX2 promoter-
87 driven lentivirus-based approach to select cells expressing CDX2 (Extended Data Fig.2a-c and
88 methods). Based on the transduction efficiency and mCherry fluorescence, out of three candidates,
89 a sequence containing 612bps of CDX2 promoter (promoter 1) was selected (Extended Data
90 Fig.2d-g, also see supplemental data) and within the multiplicities of infection (MOI) ranging from
91 20-100 MOI (Extended Data Fig.2h-q), the 50MOI range was further chosen.

92 Following initial culturing, chorionic cells from term placentas were transduced with the
93 chosen lentivirus to select CDX2mCherry positive cells (**Fig. 2a**). Flow cytometry-based sorting
94 of transduced chorionic cells from various placentas revealed that the frequency of CDX2mCherry
95 cells ranged from 1.2% to 30% with a mean frequency of 8.91 ± 1.63% (**Fig. 2b**). Immunostaining
96 demonstrated that the majority of mCherry signals (red) co-localized with nuclear CDX2 (green,
97 **Fig. 2c**) validating endogenous CDX2 expression. To understand whether CDX2 cells can self-
98 renew in a similar fashion to stem/progenitor cells, we examined the clonal proliferation of single
99 isolated CDX2 cells for a period of 14 days. CDX2 cells demonstrated a robust clonal efficiency
100 (54.1 ± 6.78%) as analyzed (**Fig. 2d-f**). Interestingly, mCherry-negative chorionic cells also
101 showed the ability of clonal proliferation (44 ± 11.45%) albeit to a lower extent than CDX2 cells.
102 *In vitro* expansion of CDX2 cells showed the retention of mCherry fluorescence through passages
103 (**Fig.2g-i**) with a significant increase in cell yield after each passage until approximately 1 million
104 cells were generated by passage 6 based on input cell number (**Fig.2g**). This suggests that CDX2
105 cells are amenable to *in vitro* expansion in culture. Response to chemotactic signaling is another
106 key feature of stem/progenitor cells. We examined CDX2 cells for their ability to migrate to
107 chemokine stromal-derived factor 1 α (SDF1) using a transwell migration assay. Before assessing
108 chemotaxis, we preconditioned one group of CDX2 cells with 1uM of AMD3100, an antagonist
109 of SDF1 receptor CXCR4. Under normal conditions, CDX2 cells exhibited a significantly higher
110 migration (22.4 ± 2.68%) to chemokine SDF1 compared to mCherry-negative cells (12.62 ±
111 2.11%, **Fig.2j**). Despite the presence of SDF1 in the lower well, blocking of CXCR4 using
112 AMD3100 significantly reduced the ability of these cells to migrate. Overall, the chemotaxis
113 response of CDX2 cells was significantly higher and our data show that this ability may be partly
114 mediated via a functional SDF1-CXCR4 axis. In sum, these data demonstrate that CDX2 cells

115 possess key features of stem/progenitor cells as these cells clonally proliferate, are amenable to *in*
116 *vitro* expansion, and possess significantly higher homing potential *in vitro*.

117 **CDX2 cells possess transcriptomic signatures for cardiovascular development, cell survival,**
118 **and immune modulation**

119 To decipher the functional repertoire within human placental CDX2 cells, we examined
120 transcript abundance using ultra-low input RNA sequencing. CDX2 is involved in trophectoderm
121 development leading to trophoblast-mediated placentation, whereas embryonic stem cells are
122 derived from the inner cell mass that significantly downregulated CDX2 expression. Hence, we
123 included an undifferentiated embryonic cell line (hESCs) as a control, along with the mCherry-
124 negative cells which were not enriched for CDX2 at the time of isolation. Using the DESeq2
125 binomial tool, a comparison of differentially expressed genes (DEGs) showed that approximately
126 1065 genes were upregulated (154 genes downregulated) in CDX2 cells compared with hESCs.
127 Meanwhile, 46 genes were found to be upregulated (529 genes showing downregulation) in CDX2
128 cells when compared to mCherry-negative cells (Extended Data Table 1).

129 The top 30 DEGs across individual samples in a bi-clustering heat map in comparison with
130 hESCs are presented in **Fig. 3a**. The functional pathways in which the differentially expressed
131 genes were involved revealed tissue organization, differentiation, angiogenesis, cell survival, and
132 cardiac development (**Fig. 3b**). The highlighted genes (**Fig. 3a**) upregulated in CDX2 cells (and
133 seen downregulated in hESCs involved TBX3 and NR2F2, which are specifically involved in
134 mesoderm commitment, cardiogenesis, and congenital heart development. The downregulated
135 genes in CDX2 cells involved pluripotency markers, including POU5F1, FOXD3AS1,
136 CLAUDN6, PHC1, and others, as shown in **Fig. 3a**, lowering concerns of tumorigenicity, unlike
137 hESCs or iPSC cells. Gene ontology analyses also corresponded to functions related to immune

138 modulation, and angiogenesis (**Fig. 3b**). Interestingly, migration and chemotaxis are the other key
139 features upregulated in CDX2 cells, which we have functionally demonstrated above.

140 Examining the transcriptome of mCherry-negative cells further, we noted an upregulated
141 expression of genes involved in immune activation and inflammatory responses. Genes such as
142 RAB44, a member of the Ras family of oncogenes, are involved in immune cell activation. Other
143 immune activation response genes, including EPX, CD80 (a potent immune cell marker in T and
144 B cell activation), and acute phase genes ORM1, HP, and APOA2 (involved in HDL metabolism
145 and atherosclerotic burden) were upregulated in mCherry-negative cells (**Fig. 3c, d**). Gene
146 ontology analyses showed cardiac and vascular functional features in CDX2 cells (**Fig. 3b**).
147 Vasculogenesis-related genes were differentially expressed in CDX2 cells, especially PECAM1
148 (CD31). Other genes present included VE-cadherin (CDH5), von Willebrand Factor (vWF), and
149 ACTA2 (**Fig. 3e**), which specify the angiogenic/vascular program. Pathways and genes involved
150 in endothelial-to-mesenchymal (EndMT) transition like SNAI2, KLF4, YAP1, VCAN (Versican),
151 EGFR, CD44, TGFB2, and BMP4 that are implicated in valvular development were found to be
152 significantly upregulated in CDX2mCherry cells when compared with mCherry-negative cells
153 (Extended Data Fig.3). Interestingly, a remarkable cluster of key genes implicated in mesodermal
154 and cardiac commitment (HAND2, DKK1, STC2, FHL1, ITGA, MYOCD, EDN1, and TGFB2)
155 was preferentially upregulated in CDX2 cells (**Fig. 3f**). These gene signatures are implicated in
156 cardiac differentiation and cardiac tissue growth in the fetal and adult heart. CDX2 cells still
157 retained a significant upregulation of mesodermal, cardiac, and sarcomere organization genes,
158 including FHL1, STC2, DKK1, TGFB2, and EDN1 (**Fig. 3f**) in comparison to mCherry-negative
159 cells. These data also suggest that, in comparison to undifferentiated ES cells, chorionic CDX2

160 cells are farther along the mesodermal/cardiac commitment pathway. These transcriptomics results
161 suggest that CDX2mCherry cells are enriched for a committed cardiovascular gene signature.

162 **CDX2 cells are angiogenic and differentiate into functional endothelial cells**

163 In line with the transcriptome analysis, we also noticed that a subpopulation of CDX2 cells
164 develops endothelial vessel-like structures (27.3±5.6%) and express endothelial markers
165 PECAM1(CD31) and von Willebrand factor (vWF) when co-cultured with murine neonatal
166 cardiomyocytes (**Fig 4a-c**). In addition, under feeder-free conditions, CDX2 cells uniformly
167 expressed smooth muscle marker (SM22α, 95.5 ± 1.59%) supporting a mesodermal phenotype
168 (**Fig. 4d-e**). To examine functional angiogenesis, we next assessed whether CDX2 cells could form
169 an angiogenic network *in vitro*. Endothelial cells recapitulate angiogenesis by forming capillary-
170 like structures when seeded onto basement membrane-like surfaces such as Matrigel. CDX2 cells
171 displayed tubular extension and loop formation within 3 h and formed endothelial-like networks
172 after 6 h. (**Fig. 4f and g**, **Movie1,**). mCherry-negative cells displayed a less organized and flattened
173 morphology (**Fig. 4h, i**), of network pattern in comparison to CDX2 cells under identical
174 conditions. HUVEC served as positive control showing a robust tubular network at both 3h and
175 6h time points (**Fig.4j and k**, **Movie2**), while unfractionated chorionic cells did not show any
176 events of tube formation (**Fig. 4l, 4m**). Quantification of the meshes[18] within the endothelial
177 network showed a higher mesh area in CDX2 cells and displayed a higher trend in the branch
178 length, segments, and nodes as noted (**Fig.4 o-s**). Ac-LDL uptake serves as the golden standard of
179 functional endothelium via receptor-mediated endocytosis. Therefore, CDX2mCherry cells
180 primed with endothelial media containing 10ng/mL VEGF were subjected to Ac-LDL for 4 hours
181 and Ac-LDL uptake was confirmed (**Fig 4n**, green). These data suggest that CDX2 cells can
182 undergo endothelial differentiation and form functional endothelium.

183 **CDX2 cells robustly differentiate into spontaneously beating cardiomyocytes**

184 We further examined CDX2 cells for cardiomyogenesis using a neonatal cardiomyocyte
185 feeder system, as described in our murine studies[17]. CDX2mCherry cells from term healthy
186 chorions were plated on beating neonatal murine cardiomyocyte feeders, which provide a niche
187 conducive to differentiation in the absence of additional exogenous growth factors or inducers.
188 Our previous studies successfully used this culture system for proof of concept testing. Isolated
189 CDX2 cells were plated and monitored on neonatal myocyte feeders. Live cell imaging showed
190 CDX2 cells formed beating organoid-like clusters as early as 4-5 days in culture (**Movie3** and **Fig.**
191 **5a**). Within two weeks, these clusters adhered and spread to display an elongated phenotype while
192 they continued to beat in culture (**Fig. 5b** and**Movie4**). After 4 weeks of culture, immunostaining
193 for human-specific sarcomeric actinin, in combination with cardiac troponin T (cTnT- detect both
194 mouse and human myocytes), demonstrated that CDX2-derived cardiomyocytes robustly
195 expressed cardiac sarcomeric proteins with striations **(Fig. 5c-e'**). On the contrary, the mCherry-
196 negative cells displayed a much lower cardiogenic capacity when cultured in identical conditions,
197 further corroborating our transcriptomics data and supporting cardiogenic ability in CDX2 cells
198 (Extended Data Fig.4). Approximately 71.11±12.15% of input CDX2 cells differentiated into
199 cardiomyocytes (**Fig. 5f**) and these data demonstrate that placental CDX2 cells are cardiogenic
200 and differentiate into spontaneously beating cardiomyocytes in culture. These findings have
201 significant translational implications, and we envision multipotent human placenta-derived CDX2
202 cells as an innovative approach for cardiovascular regeneration.

203 **Discussion**

204 In this study, we have demonstrated that CDX2-expressing cells isolated from term human
205 placentas possess key characteristics of stem/progenitor cells and differentiate into cardiovascular

206 lineages in addition to migrating to the chemokine SDF1α. CDX2 is essential in embryonic
207 development and is found in the trophectoderm, which in turn regulates placentation. During
208 embryonic development, the placenta and fetal heart progress in parallel (placenta-heart axis) with
209 the placenta regulating fetal cardiomyocyte proliferation, signifying a key functional association
210 between these organs[8-10]. Our findings lend credence to such a scenario as placenta-derived CDX2
211 cells are uniquely poised to drive cardiovascular commitment and can now be viewed as a cellular
212 target for cardiogenesis.

213 Various cell sources for therapeutic approaches have been studied in cardiac regeneration
214 for decades, and the safety of such approaches has been established in clinical trials. However,
215 finding an ideal and readily accessible cell type that can give rise to cardiovascular cells, aside
216 from ESCs and iPSCs, has proven difficult. Prenatal placental cells, particularly placental
217 mesenchymal stem cells (PMSCs) and amniotic epithelial cells (AECs) have anti-inflammatory,
218 angiogenic, and paracrine mechanisms that are beneficial for cardiac regenerative approaches but
219 have not been shown to generate *de novo* cardiomyocytes[19-21]. On the other hand, endogenous
220 trophoblast progenitors in the placenta have not been explored for their differentiation into other
221 cell types. Our previous studies demonstrated the potential of murine Cdx2 lineage cells in the
222 placenta to migrate to the sites of cardiac injury and produce new cardiovascular cells, significantly
223 improving cardiac function[17]. In a paradigmatic shift, we have now shown that multipotent human
224 CDX2 cells are retained in the cytotrophoblasts of the human placenta through term. Our
225 observation of the localization of CDX2 to the cytotrophoblast region is consistent with the studies
226 of the early-gestational placenta [21.] Cytotrophoblast cells are proliferative stem cells that migrate
227 and invade maternal spiral arteries during placentation[22]. Similarly, we observed that CDX2 cells
228 from term placenta, expressed villous trophoblast markers, exhibit clonal proliferation and

229 migration supporting the stem/progenitor characteristics suitable for cardiac regenerative
230 approaches.

231 CDX2 cells and mCherry-negative cell populations were examined in our studies using a
232 lentivirus-based isolation method. Even though sourced from healthy placentas, differences in
233 proliferation among various samples existed. We are presently targeting the kinetics of
234 proliferation and differentiation at the single-cell level and this will further provide valuable clues
235 that can resolve cellular heterogeneity within placenta samples. In this study, we have also
236 incorporated a sizable group of healthy donors of varied races which included 106 placentas, to
237 account for any biological diversity. This approach may facilitate a more inclusive analysis as the
238 placenta samples are representative of a broader population. The selection of cells that were
239 CDX2mCherry positive also made it easier to study the functional competency of mCherry-
240 negative counterparts from the same anatomical region of the chorion. Even though clonal
241 efficiency was not drastically different, with this closer comparison, we could conclusively
242 determine that CDX2 cells have significantly enhanced cardiovascular capability compared with
243 mCherry-negative cells. Similarly, the transcriptomic signature of mCherry-negative cells
244 displayed a lesser extent of mesodermal differentiation when compared to CDX2 cells. With the
245 additional hESC stem cell control, we also observed that CDX2 cells significantly upregulated
246 chemotaxis, migration, and cardiovascular gene signatures in both comparisons.

247 Consistent with transcript analyses, human CDX2 cells generated spontaneously beating
248 cardiomyocyte cell clusters within 5 days followed by approximately 70% of CDX2 cells
249 differentiating into cardiomyocytes on neonatal murine cardiomyocyte feeders. Remarkably, the
250 time frame for the emergence of beating clusters was relatively shorter in CDX2 cells contrary to
251 other inductive co-culture approaches or standard protocols using pluripotent stem cells, which

252 demonstrate the onset of beating within 8–12 days[23-25]. It is conceivable that this is because of the
253 enriched pre-existing cardiogenic transcriptome present in the isolated CDX2 cells. These findings
254 suggest that CDX2 cells may be a promising population for generating cardiomyocytes in a shorter
255 time frame, which could have significant implications for regenerative medicine.

256 Since the placenta becomes an increasingly vascular organ during the course of gestation,
257 cells from the placenta can be highly angiogenic. As we noted from the data from our trancriptomic
258 analyses, endothelial tube formation from CDX2 cells suggested a strong angiogenic commitment
259 and Ac-LDL uptake confirmed that the CDX2-derived endothelial cells are functional.
260 Angiogenesis is a crucial feature in cell therapy and cardiac repair, as the engraftment of adoptively
261 transferred cells into the surrounding microenvironment is highly dependent on establishing *de*
262 *novo* vasculature. Interestingly, angiogenesis and the invasive nature of trophoblast cells are
263 interlinked as the migration potential of trophoblast cells directs endothelialization/angiogenesis
264 during placentation [26,27.] On the other hand, SDF1-mediated chemotaxis is further involved in stem
265 cell-mediated homing for regeneration[28-30] and CDX2 cells demonstrated significantly higher
266 SDF1-mediated migration compared to our two control populations. Our findings demonstrate the
267 functional competency of CDX2 cells from several angles critical to the development of allogeneic
268 cell therapy, making them a promising cell population for further therapeutic applications.

269 The most exciting outcome of these studies is that a new progenitor cell type has been
270 identified from a limitless source (term placenta) that differentiates into spontaneously beating
271 cardiomyocytes as well as functional vascular cells *in vitro*, thus providing a foundation for more
272 precision-guided clinical trials of cardiac regeneration.

References

1 Trounson, A. & McDonald, C. Stem Cell Therapies in Clinical Trials: Progress and Challenges. *Cell Stem Cell* **17**, 11-22 (2015). https://doi.org/10.1016/j.stem.2015.06.007

2 Xin, M., Olson, E. N. & Bassel-Duby, R. Mending broken hearts: cardiac development as a basis for adult heart regeneration and repair. *Nat Rev Mol Cell Biol* **14**, 529-541 (2013). https://doi.org/10.1038/nrm3619 nrm3619 [pii]

3 Martinez, J., Zoretic, S., Moreira, A. & Moreira, A. Safety and efficacy of cell therapies in pediatric heart disease: a systematic review and meta-analysis. *Stem Cell Res Ther* **11**, 272 (2020). https://doi.org/10.1186/s13287-020-01764-x

4 Cambria, E. *et al.* Translational cardiac stem cell therapy: advancing from first-generation to next-generation cell types. *NPJ Regen Med* **2**, 17 (2017). https://doi.org/10.1038/s41536-017-0024-1

5 Sultana, N. *et al.* Resident c-kit(+) cells in the heart are not cardiac stem cells. *Nat Commun* **6**, 8701 (2015). https://doi.org/10.1038/ncomms9701

6 Li, Y. *et al.* Genetic Lineage Tracing of Nonmyocyte Population by Dual Recombinases. *Circulation* **138**, 793-805 (2018). https://doi.org/10.1161/CIRCULATIONAHA.118.034250

7 He, L., Nguyen, N. B., Ardehali, R. & Zhou, B. Heart Regeneration by Endogenous Stem Cells and Cardiomyocyte Proliferation: Controversy, Fallacy, and Progress. *Circulation* **142**, 275-291 (2020). https://doi.org/10.1161/CIRCULATIONAHA.119.045566

8 Burton, G. J. & Jauniaux, E. Development of the Human Placenta and Fetal Heart: Synergic or Independent? *Front Physiol* **9**, 373 (2018). https://doi.org/10.3389/fphys.2018.00373

296 9 Mahadevan, A., Tipler, A. & Jones, H. Shared developmental pathways of the placenta
297 and fetal heart. *Placenta* (2022). https://doi.org/10.1016/j.placenta.2022.12.006
298 10 Ward, E. J. *et al.* Placental Inflammation Leads to Abnormal Embryonic Heart
299 Development. *Circulation* (2022).
300 https://doi.org/10.1161/CIRCULATIONAHA.122.061934
301 11 Shen, H. *et al.* Extracardiac control of embryonic cardiomyocyte proliferation and
302 ventricular wall expansion. *Cardiovasc Res* **105**, 271-278 (2015).
303 https://doi.org/10.1093/cvr/cvu269
304 12 Felker, G. M. *et al.* Underlying causes and long-term survival in patients with initially
305 unexplained cardiomyopathy. *N Engl J Med* **342**, 1077-1084 (2000).
306 https://doi.org/10.1056/NEJM200004133421502
307 13 Antoniadou, E. & David, A. L. Placental stem cells. *Best Pract Res Clin Obstet Gynaecol*
308 **31**, 13-29 (2016). https://doi.org/10.1016/j.bpobgyn.2015.08.014
309 14 Maltepe, E., Bakardjiev, A. I. & Fisher, S. J. The placenta: transcriptional, epigenetic,
310 and physiological integration during development. *J Clin Invest* **120**, 1016-1025 (2010).
311 https://doi.org/10.1172/JCI41211
312 15 Niwa, H. *et al.* Interaction between Oct3/4 and Cdx2 determines trophectoderm
313 differentiation. *Cell* **123**, 917-929 (2005). https://doi.org/10.1016/j.cell.2005.08.040
314 16 Kara, R. J. *et al.* Fetal cells traffic to injured maternal myocardium and undergo cardiac
315 differentiation. *Circ Res* **110**, 82-93 (2012).
316 https://doi.org/10.1161/CIRCRESAHA.111.249037CIRCRESAHA.111.249037 [pii]

317 17 Vadakke-Madathil, S. *et al.* Multipotent fetal-derived Cdx2 cells from placenta
318 regenerate the heart. *Proc Natl Acad Sci U S A* **116**, 11786-11795 (2019).
319 https://doi.org/10.1073/pnas.1811827116
320 18 Carpentier, G. *et al.* Angiogenesis Analyzer for ImageJ - A comparative morphometric
321 analysis of "Endothelial Tube Formation Assay" and "Fibrin Bead Assay". *Sci Rep* **10**,
322 11568 (2020). https://doi.org/10.1038/s41598-020-67289-8
323 19 Gorodetsky, R. & Aicher, W. K. Allogenic Use of Human Placenta-Derived Stromal
324 Cells as a Highly Active Subtype of Mesenchymal Stromal Cells for Cell-Based
325 Therapies. *Int J Mol Sci* **22** (2021). https://doi.org/10.3390/ijms22105302
326 20 Song, Y. S. *et al.* Transplanted Human Amniotic Epithelial Cells Secrete Paracrine
327 Proangiogenic Cytokines in Rat Model of Myocardial Infarction. *Cell Transplant* **24**,
328 2055-2064 (2015). https://doi.org/10.3727/096368914X685609
329 21 Soncin, F. *et al.* Comparative analysis of mouse and human placentae across gestation
330 reveals species-specific regulators of placental development. *Development* **145** (2018).
331 https://doi.org/10.1242/dev.156273
332 22 Lyall, F., Bulmer, J. N., Kelly, H., Duffie, E. & Robson, S. C. Human trophoblast
333 invasion and spiral artery transformation: the role of nitric oxide. *Am J Pathol* **154**, 1105-
334 1114 (1999). https://doi.org/10.1016/S0002-9440(10)65363-1
335 23 Lian, X. *et al.* Robust cardiomyocyte differentiation from human pluripotent stem cells
336 via temporal modulation of canonical Wnt signaling. *Proc Natl Acad Sci U S A* **109**,
337 E1848-1857 (2012). https://doi.org/10.1073/pnas.1200250109

338 24 Balafkan, N. *et al.* A method for differentiating human induced pluripotent stem cells
339 toward functional cardiomyocytes in 96-well microplates. *Sci Rep* **10**, 18498 (2020).
340 https://doi.org/10.1038/s41598-020-73656-2
341 25 Mummery, C. L. *et al.* Differentiation of human embryonic stem cells and induced
342 pluripotent stem cells to cardiomyocytes: a methods overview. *Circ Res* **111**, 344-358
343 (2012). https://doi.org/10.1161/CIRCRESAHA.110.227512
344 26 Piera-Velazquez, S. & Jimenez, S. A. Endothelial to Mesenchymal Transition: Role in
345 Physiology and in the Pathogenesis of Human Diseases. *Physiol Rev* **99**, 1281-1324
346 (2019). https://doi.org/10.1152/physrev.00021.2018
347 27 Alvandi, Z. & Bischoff, J. Endothelial-Mesenchymal Transition in Cardiovascular
348 Disease. *Arterioscler Thromb Vasc Biol* **41**, 2357-2369 (2021).
349 https://doi.org/10.1161/ATVBAHA.121.313788
350 28 Lapidot, T. & Kollet, O. The essential roles of the chemokine SDF-1 and its receptor
351 CXCR4 in human stem cell homing and repopulation of transplanted immune-deficient
352 NOD/SCID and NOD/SCID/B2m(null) mice. *Leukemia* **16**, 1992-2003 (2002).
353 https://doi.org/10.1038/sj.leu.2402684
354 29 Lau, T. T. & Wang, D. A. Stromal cell-derived factor-1 (SDF-1): homing factor for
355 engineered regenerative medicine. *Expert Opin Biol Ther* **11**, 189-197 (2011).
356 https://doi.org/10.1517/14712598.2011.546338
357 30 Song, M. *et al.* Regeneration of chronic myocardial infarction by injectable hydrogels
358 containing stem cell homing factor SDF-1 and angiogenic peptide Ac-SDKP.
359 *Biomaterials* **35**, 2436-2445 (2014). https://doi.org/10.1016/j.biomaterials.2013.12.011

360 **Main Figures**

Figure 1

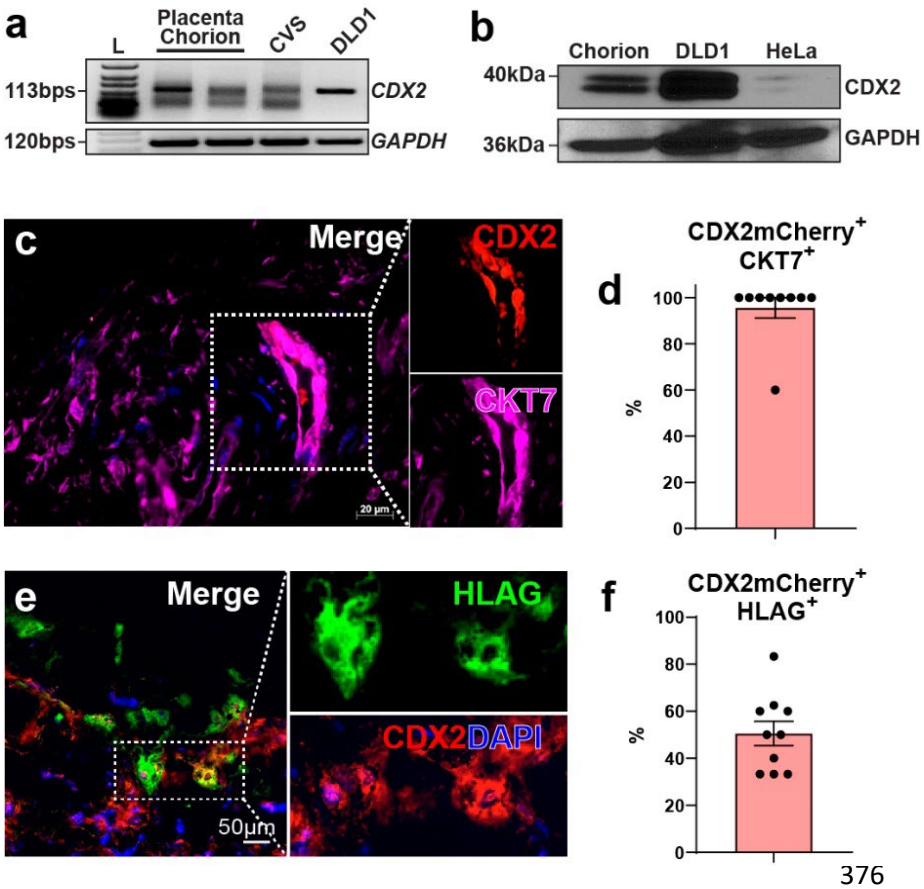

376

377 **Figure 1: CDX2 expression found to be enriched in term human chorionic tissues**. (a) CDX2
378 mRNA expression in the first-trimester chorionic villous sample and term chorion from the healthy
379 placenta. L=DNA ladder (Gene Ruler ultralow DNA ladder). Human adenocarcinoma cell line
380 DLD1 displays a higher expression of CDX2 and hence served as a positive control. Gapdh served
381 as an internal control. (b) Western blot analyses on term healthy chorionic samples (80µg
382 protein/sample) showed CDX2 protein (40KDa) with a doublet pattern indicative of the alternate
383 splicing. DLD1 served as a positive control, while HeLa cells as a control with low endogenous
384 CDX2 expression. (c) Immunofluorescence detection of CDX2 in term chorion showed that CDX2

385 (clone CDX88-red) is mainly expressed in the villi region encompassing the cytotrophoblast cells
386 and co-express trophoblast marker Cytokeratin 7 (pink -CKT7). (d) Quantification of tissue
387 sections showing the percentage of CDX2 cells co-expressing CKT7. (e) Approximately 50%
388 (50.5±5.0%) of CDX2 cells co-expressed HLA-G, a crucial marker identifying extravillous
389 trophoblast progenitors in the placenta. n=3 independent placental samples wherein 3 different
390 ROIs from each section were screened.

391

Figure 2

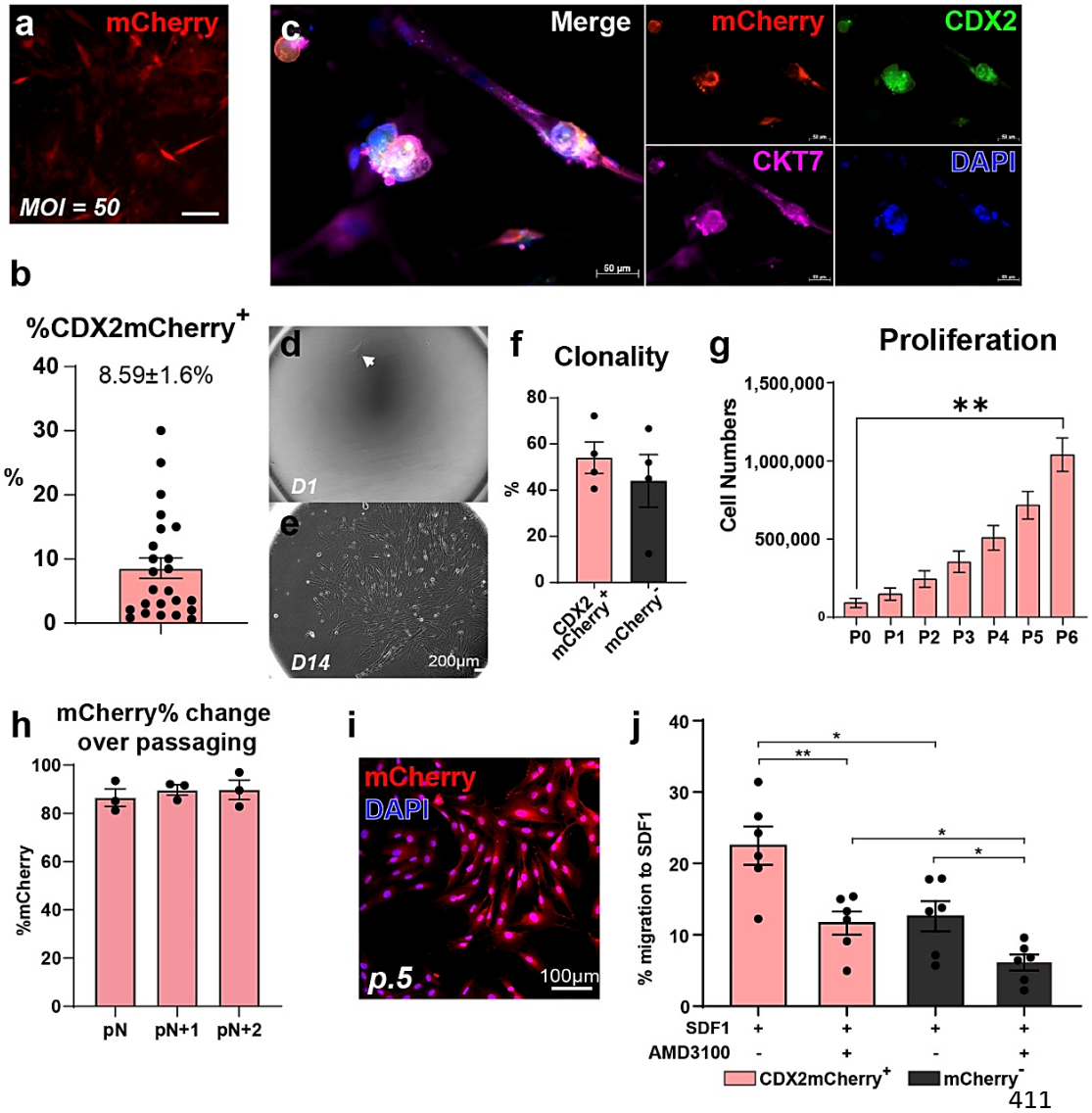

411

412 **Figure 2: CDX2 cell isolation, proliferation, and homing *in vitro*** (a) CDX2 lenti mCherry was
413 used to transduce chorionic cells (50 MOI), and cells expressing CDX2 displayed mCherry
414 fluorescence. (b) Flow cytometry-based isolation of mCherry+ cells and quantification of
415 CDX2mCherry cells from various placentas. Data are presented as mean ± SEM (n=25
416 independent samples). (c) The specificity of the lentivirus-based selection of CDX2 cells was
417 validated using CDX2mAb (CDX-88clone). Co-localization of mCherry fluorescence with CDX2

418 antibody (Alexa 488) and trophoblast marker Cytokeratin 7 (CKT7-pink is shown (d,e)
419 Representative phase contrast image showing clonal proliferation CDX2 cells on day 14 (e)
420 compared to day 1 (d) in culture. (f) Clonal efficiency was analyzed on day 14 and found to be
421 54.1 ± 6.78% in CDX2 cells versus 44 ± 11.45% in mCherry negative cells. Data are presented as
422 mean ± SEM (n=4 independent samples) (g) Quantification of mCherry cells after expansion
423 showed a significant increase of up to 1 million cells by passage 6 compared to day 0 of isolation,
424 Data represented as mean±SEM (n=3, *$p<0.05$, **$p<0.01$) (h) Retention of mCherry expression
425 over the various passages as analyzed by flow cytometry and (i) a representative image at p5. (j)
426 In vitro homing of CDX2 cells and mCherry negative cells to chemokine SDF1 is dependent on
427 the CXCR4 axis. CDX2 cells show significantly higher migration in both conditions compared to
428 mCherry-negative cells. Data are presented as mean ± SEM (n=3 biological replicates comprising
429 3 independent samples *$p<0.05$, **$p<0.01$).

430

Figure 3

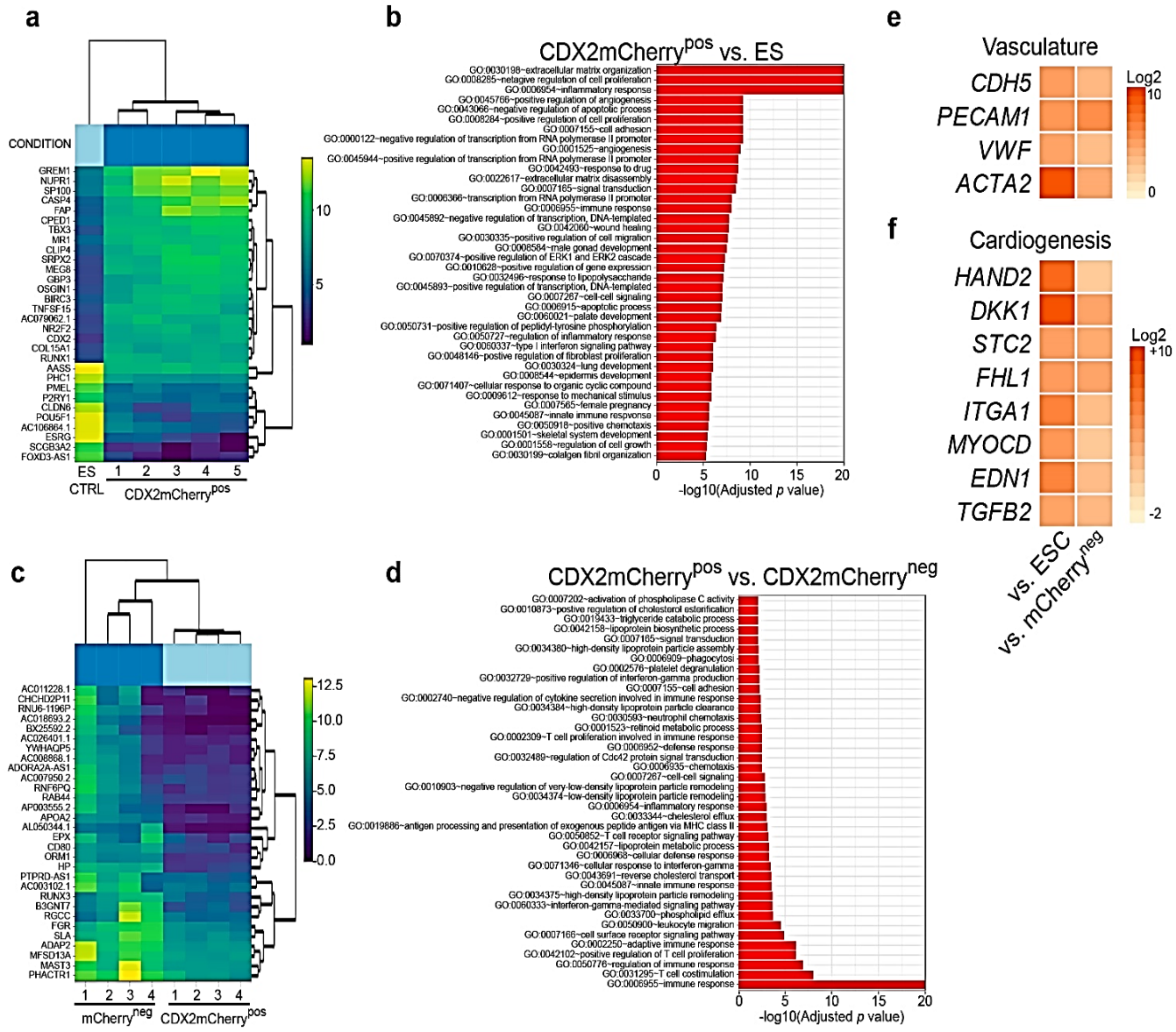

431 **Figure 3: Ultra-low input RNAseq analyses on CDX2 cells versus hESCs and mCherry**
432 **negative cells** (a) Bi-clustering heat map showing the expression profile of the top 30 differentially
433 expressed genes in CDX2 cells (labeled 1-5 right) versus hESCs (H9 ES ctrl pooled extreme left).
434 Genes were sorted by their adjusted p-value by plotting the log2 transformed expression values.
435 The yellow-green color code indicates the upregulated and the blue-gray color code indicates the

436 downregulated genes across the samples. CDX2 cells showed upregulated mesoderm commitment
437 genes including NR2F2 and TBX3 (cardiogenic) while downregulating pluripotent markers
438 CLDN6, POU5F1, ESRG (b) Further, differentially expressed genes (up to 40) vs. hES cells show
439 gene ontology terms enriched with an adjusted p-value less than 0.05 corresponding to functions
440 related to angiogenesis, immune modulation, migration, and chemotaxis. (c) A bi-clustering heat
441 map with the top 30 differentially expressed genes showing the upregulated function of
442 inflammatory response and immune genes in mCherry negative cells (n=4 independent samples in
443 each group) (d) GO analyses demonstrated upregulation of functional pathways including T cell
444 proliferation, MHC class II antigen processing, and presentation, IFN gamma mediated signaling,
445 and cholesterol biosynthesis in mCherry negative cells. (e,f) CDX2 cells displayed enriched
446 transcriptomes reflecting cardiovascular development. Vascular genes like PECAM1, VE-
447 cadherin *(*CDH5*),* and smooth muscle actin *(*ACAT2*)* were upregulated in CDX2 cells in
448 comparison to hES cells and mCherry negative control samples. (f) Genes associated with cardiac
449 development including HAND2, DKK1, STC2, FHL1*,* ITGA1, MYOCD EDN1, and TGFB2
450 showed preferential upregulation in CDX2 cells.

Figure 4

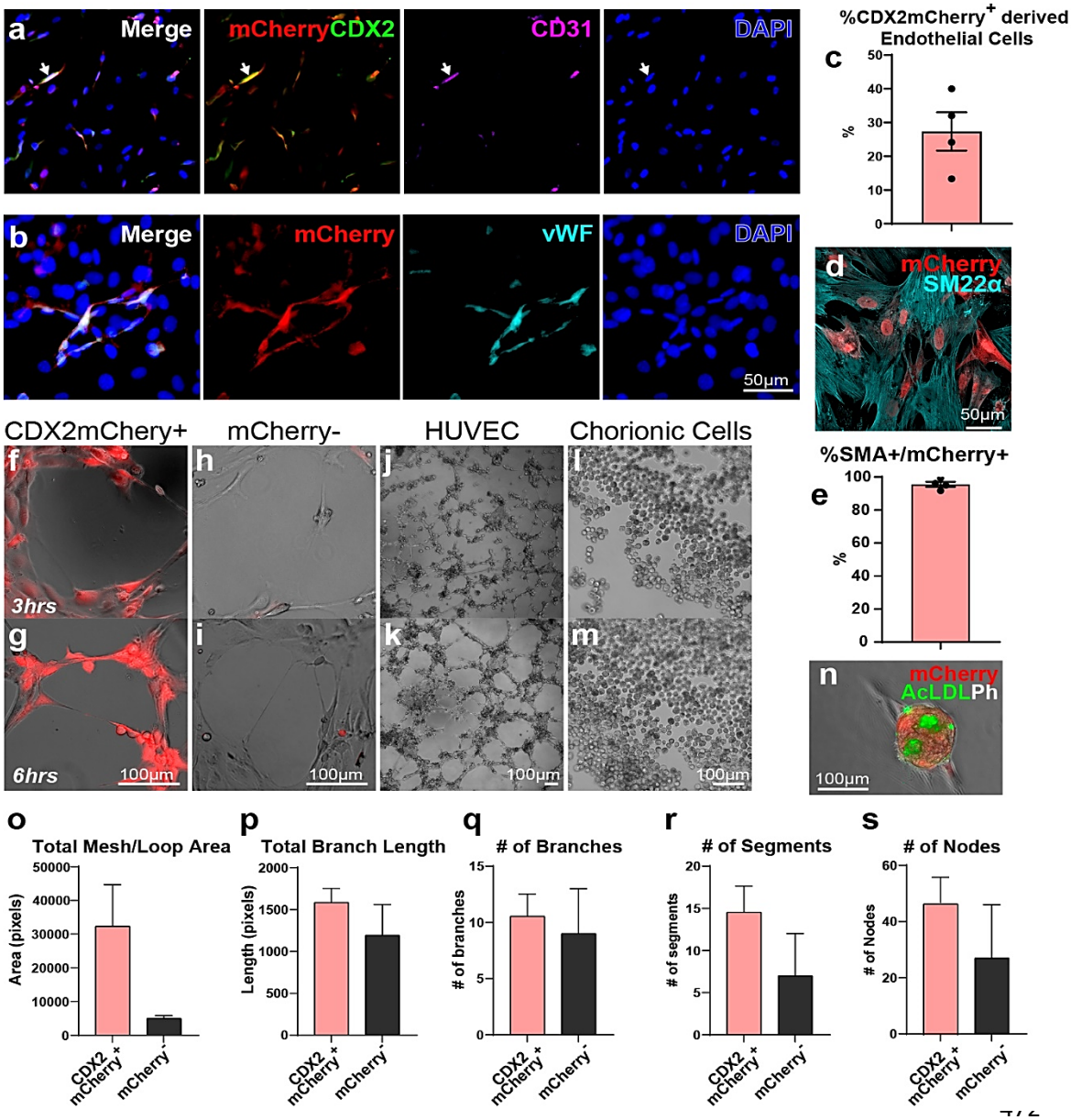

473 **Figure 4: CDX2 cells are angiogenic and display endothelial tube formation *in vitro*** (a) Subset
474 of CDX2mCherry cells (red) expressed vascular lineage marker CD31 (pink) and further gave rise
475 to blood vessel-like assembly (and stained positive for endothelial marker von Willebrand Factor
476 (vWF-green) upon co-culture with neonatal cardiomyocytes (b, c). Data represented as
477 mean±SEM of four independent samples (n=4). (d,e) CDX2mCherry cells also expressed smooth

478 muscle marker SM22α upon feeder-free culture using IMDM+10%FBS (f,g) Endothelial tube
479 formation by CDX2mCherry cells on matrigel in 3hrs and the formation of endothelial-like
480 networks within 6hrs, also refer to movie S1.(h, i) mCherry negative cells showing networks albeit
481 not as intact and optimal as their CDX2mCherry counterpart on matrigel. (j,k) Human umbilical
482 vein endothelial cells (HUVEC) served as a positive control, also refer to movie S2 (l,m) Total
483 chorionic cells from the placenta did not exhibit endothelial tube formation at both time points. (n)
484 Ac-LDL (Alexa-488) uptake by primed (M200 medium +LSGS+ 10ng/mL VEGF)
485 CDX2mCherry cells suggesting the formation of a functionally active endothelium (o-s)
486 Quantification of the endothelial network using ImageJ software with angiogenesis analyzer
487 showed a higher endothelial loop like area, branching segments compared to mCherry negative
488 cells (n=5 independent CDX2mCherry positive and n=2 independent mCherry negative samples
489 with biological triplicates per assay).

Figure 5

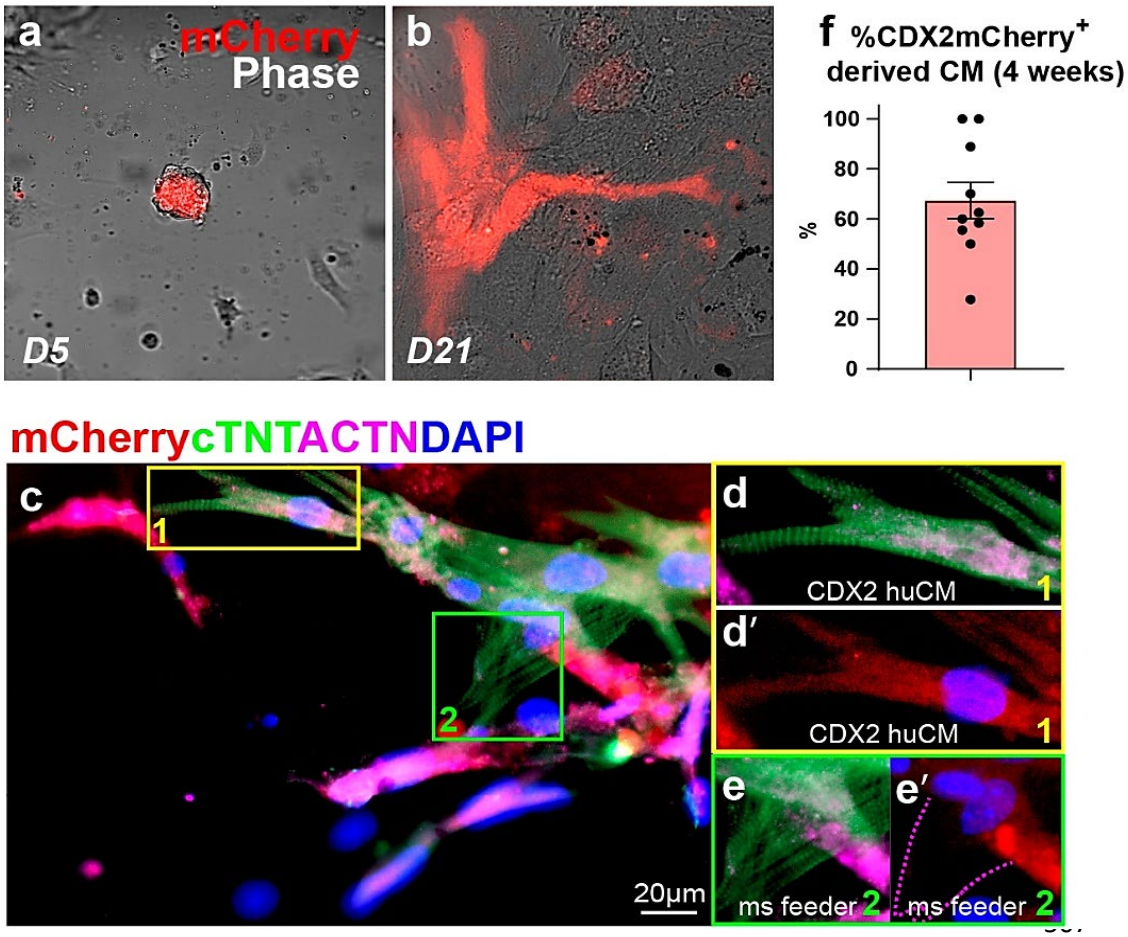

Figure 5: CDX2 cells differentiate into spontaneously beating cardiomyocytes in co-culture with neonatal myocyte feeder (a) Snapshot of a beating CDX2mcherry cell cluster on day 5 on co-culture with murine neonatal cardiomyocytes feeder (non-mCherry-gray cells in the background), also see movie S3. (b) Snapshot of beating adhered and elongated CDX2mCherry cardiomyocytes 3 weeks in culture (movie S4). (c) Most of the CDX2mCherry cells-derived cardiomyocytes (mCherry-red) stain positive for human cardiac sarcomeric actinin (pink-Alexa 647) and cardiac troponin T (cTnT-green Alexa 488). The specificity of the human actinin antibody was detected by a lack of staining on murine feeder myocytes in the background, while cTnT (green) detects both mouse and human cardiomyocytes. Yellow box 1 is further highlighted

517 to the right (d and d') showing the striated sarcomeres visible on human CDX2 mCherry-derived
518 cardiomyocytes (actinin pink + cTnT green+). Meanwhile, green box 2 and the expanded panels
519 point to the endogenous murine feeder myocyte that expresses only cTnT (green) (e and e'). Nuclei
520 are counterstained using DAPI (blue). (f) Quantification revealed that approximately
521 71.11±12.15% of input CDX2 cells differentiated into cardiomyocytes as shown. Data are
522 represented as mean ± SEM (n=5 independent samples).

523 **Methods**

524 **Human subjects**

525 Pregnant women enrolled in this study ranged from to 18-45 years, were ethnically and racially
526 diverse, and reflected those served by the Maternal Fetal Medicine Practice at Mount Sinai. 189
527 patients are currently enrolled in this study. Placenta samples were collected under two cohorts. 1)
528 Mount Sinai approved IRB protocol (Study 20-0068, IF2646084), which reflects the prospective
529 cohort that has now 189 enrolled patients (including future due dates) from which 31 samples were
530 collected thus far based on the viable delivery window (weekdays 9-5 pm). Cohort 2, the de-
531 identified cohort, contained 75 fresh tissue samples under the auspices of the Institutional Biobank
532 at Mount Sinai Pathology Core facility. De-identified samples (all identifying patient information
533 was replaced by a BRP #ID) at the Biorepository Core Facility were sampled by a neonatal
534 placental pathologist. Both sample collections followed the standard protocol in order not to
535 interfere with any needed clinical assessment of the placenta and to only obtain tissue that would
536 otherwise be discarded. Unless otherwise mentioned, each experiment was performed with at least
537 three different patient samples (n=3).

538 **Placental CDX2 cell isolation**

539 Placentas were received within 30 min-120 min of delivery. Gross appearance was briefly
540 examined, including identification of the cord insertion site and disc edges. Approximately 5.0 x
541 2.0 cm rectangular area of each full-thickness disc was incised off by a surgical blade midway
542 from the cord insertion site and the disc edge, avoiding obvious sub-chorionic fibrin deposition.
543 Any remaining amnion was removed using forceps. Finally, the decidual surface was shaved using
544 a blade to minimize the maternal component. The chorionic tissue was then quickly transferred to
545 1X Hanks Balanced Salt Solution (HBSS) containing 2X penicillin and streptomycin and kept on
546 ice. The fresh tissue was rinsed thoroughly using 1X HBSS to remove blood, minced into
547 approximately $1mm^3$, pieces, and transferred to 50mL falcon conical tubes containing 2 mg/mL
548 Collagenase Type 2 (Worthington, NJ, Cat#LS0004194) and 1 mg/mL Pronase
549 (Calbiochem,Cat#53702) solution in 1X HBSS. The samples were incubated in enzyme solution
550 for 2 h at 37 °C and 5% CO_2. The tissue mixture containing the enzyme solution was gently mixed
551 every 20 min using disposable pipettes to facilitate digestion. At the end of digestion, the enzyme
552 reaction was stopped by the addition of serum, and the cell mixture was filtered using a 100-micron
553 cell strainer (Falcon, Cat#352360) and centrifuged at 1600rpm for 4 min. Red blood cells were
554 removed using 1X RBC lysis buffer (10X stock, eBioscience, Cat# 00-4300-54) by incubating the
555 cell pellet in lysis buffer (15 min, room temperature in the dark) followed by centrifugation. The
556 final cell pellet was resuspended in IMDM+10% FBS or the respective assay medium for
557 downstream experiments.

558 **Lentiviral transduction and isolation of placental CDX2 cells**

559 To select viable CDX2 cells from the total chorionic cells, we designed a lentiviral construct in
560 which the human CDX2 promoter drives mCherry fluorescence. The CDX2 gene is oriented in the

561 reverse (3'-5') sequence, and its promoter expression is not as strong as that of conventional
562 upstream promoters. Hence, we designed three different constructs using sequences spanning
563 different regions upstream of the 3' UTR, and in some cases, also spanning a fragment into the
564 start codon to include promoter region 1 (612bps), promoter region 2 (1174bps), and promoter
565 region 3 (1197bps). The downstream detection is by mCherry fluorescence and a ubiquitous CMV
566 promoter with the same vector backbone served as a control for transduction efficiency. The
567 human adenocarcinoma cell line, DLD1, served as a positive control for CDX2. Based on the
568 validation experiments (Extended Data Fig.2), CDX2 promoter 1 displayed the strongest mCherry
569 fluorescence; hence, we used lentiCDX2 (612bps) for all experiments. For transduction, chorionic
570 cells were plated at a density of 10^5 cells/24 well in IMDM+10% FBS and were allowed to adhere
571 overnight. The following day, cells were transduced with lentivirus at 50 multiplicity of infection
572 (MOI=50) viral particles per cell with8µg/mL polybrene to facilitate transduction. The plates were
573 spinoculated at 2000 rpm for 1 min and incubated at 37 °C and 5% CO_2 for 48 -72h After 48 h,
574 the medium was replaced and the cells were examined for mCherry fluorescence under a Zeiss
575 AxioObserver epifluorescence microscope; mCherry-positive and mCherry-negative populations
576 were separated using flow cytometry-based sorting using a BD Influx/IMI5L/Cytek Aurora sorter.

577 **Ultralow-input RNA sequencing**

578 Isolated CDX2mCherry cells (n=5) mCherry negative cells (n=4) and hES cells (n=2 pooled) were
579 centrifuged and 200uL Tri reagent (Thermo Fisher Scientific, USA) was added and incubated at
580 room temperature for 15 min. The samples were stored at -80°C until RNA extraction and library
581 preparation were performed. The library preparation workflow is depicted below for sequencing
582 on Illumina Hiseq (HiSeq™ 2000 Sequencing System, Illumina, Genewiz/Azenta Life Sciences).

583 **Statistical Analysis**

584 The number of biological and technical replicates is indicated in figure legends wherever
585 appropriate. Data are presented as mean ± SEM unless otherwise indicated. All
586 immunohistochemistry micrographs were quantified by ImageJ (analyze particle). For pairwise
587 comparisons, significance was determined followed by post-hoc Tukey's or Bonferoni's test to
588 conserve the inflation of the Type I error rate. An unpaired t-test was used to analyze the rest of
589 the datasets. A two-tailed alpha level of 0.05 was used, and a P value of ≤0.05 was considered
590 significant.

591 **Acknowledgments**

592 We thank Ms. Carolyn Quinn for proofreading the manuscript. We thank the Flow Cytometry Core
593 Facility, Imaging Core Facility, Biorepository and Pathology Core Facility, and Stem Cell
594 Engineering Core at the Icahn School of Medicine at Mount Sinai for technical assistance. We
595 thank Dr. Lisa Edelman (Genetics and Genomics Sciences, Mount Sinai) for kindly providing
596 chorionic villous samples for the study. This study was supported by New York Stem Cell Board
597 funds IIRP Contract C32608GG, NIH/NHLBI R01HL150345 to H.W.C and KL2
598 1KL2TR004421-01(NIH CTSA Mount Sinai) to SVM.

599 **Author Contributions**

600 S.V.M., designed and performed experiments, analyzed the data and wrote the paper. B.J.W.
601 performed experiments, analyzed the data, and organized the figures. M.O., coordinated the
602 enrollment, assisted in the processing of placental samples, and performed cell cultures. F.D.
603 examined the placenta and performed the sampling. R.B. examined the de-identified patient data
604 and provided the tissue sections. S.G. and R.S. were closely involved in coordinating the human
605 subject enrollment and assisted in the timely procurement of samples. H.W.C. conceived the study,

606 interpreted the results with all authors, and wrote the paper with S.V.M. All authors edited and
607 approved the paper.

608 **Competing Interest Declaration**

609 H.W.C the senior and co-corresponding author of this study is the inventor of an issued EU patent
610 and pending US patent owned by Icahn School of Medicine at Mount Sinai (Methods of Cardiac
611 Repair, No. 12847330.3) regarding the use of CDX2 cells for heart repair. She is also the founder
612 of a biotech VentriNova, Inc. that may benefit from the publication of the results presented
613 regarding human CDX2 cells. Although the company is still in the early stages and seeking
614 institutional financing, H.W.C. owns stock in the company.

615 **Additional Information**

616 Supplementary Information is available for this paper. Online-only methods are available for this
617 paper. Correspondence and requests for materials should be addressed to Hina Chaudhry at
618 hina.chaudhry@mssm.edu

619 **Data and code availability**

620 The new plasmids generated in this study will be made available upon publication. No unique
621 reagents were generated from this study. Bulk sequencing data will be made available in the NCBI
622 Sequencing Read Archive (SRA). De-identified placental information along with the patient's age
623 and race/ethnicity data will be available upon request.

624 **Extended Data Figures**

Figure S1

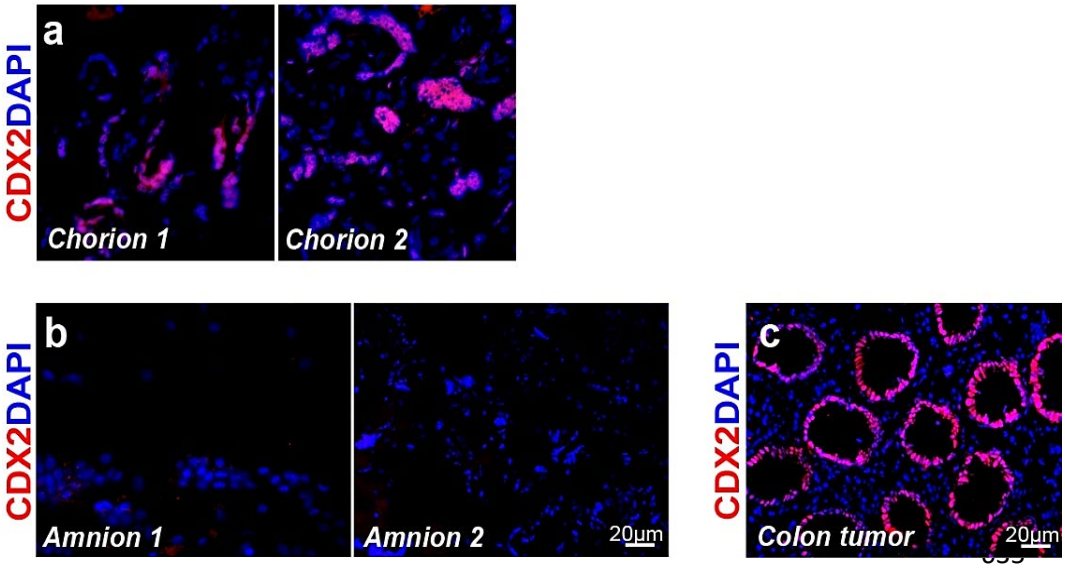

636 **Extended Data Figure 1. CDX2-expressing cells are enriched in chorionic cells in human**
637 **term placenta** (a) Chorionic tissue sections show nuclear CDX2, especially in the villous region
638 and within the cytotrophoblast, whereas amniotic tissue sections (b) showed low/lack CDX2 (red-
639 mAb Abcam CDX88-clone) expression. Images represent immunostaining from two different
640 placentas samples. (c) De-identified human colon tumor tissue sections served as positive control
641 and displayed a higher CDX2 expression.

Figure S2

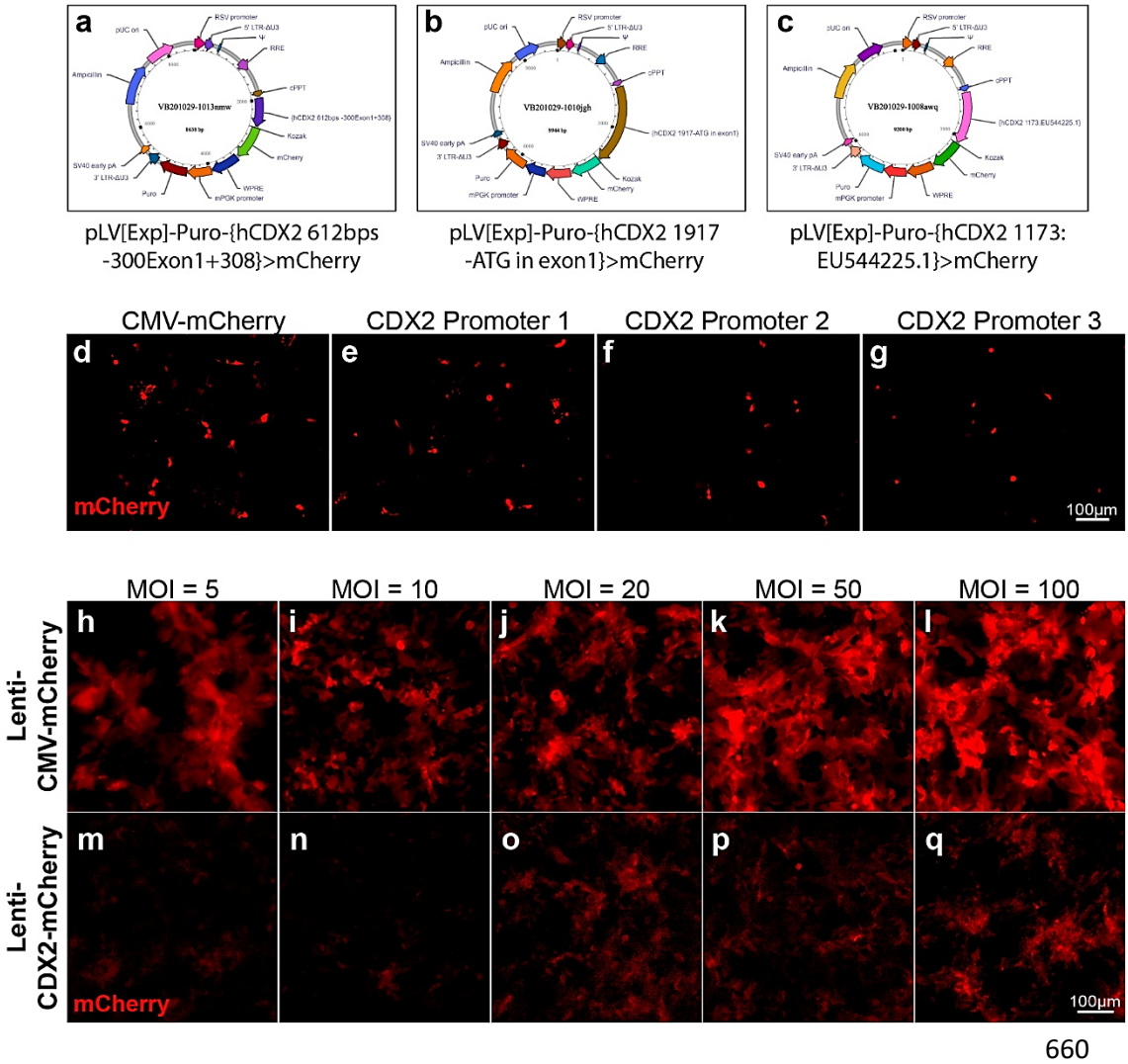

Extended Data Figure 2. Human CDX2 promoter-driven lentivirus approach (a-c) Vector map incorporating different sequence lengths of huCDX2 promoters in the vector backbone. selected promoter 1 (CDX2 612bps) designed to incorporate sequences spanning upstream exon 1 ~300 sequences and further ~308 bps into exon 1 right before the first open reading frame (ORF) at the start codon ATG site. All vector maps containing mCherry are inserted at the ORF as a fluorescence-based readout that reflects the activity of the promoter. (d-g) Human adenocarcinoma cell line DLD1 displays a higher expression of endogenous CDX2 and hence we assessed the efficiency of the designed promoters in detecting CDX2 by visualizing the mCherry fluorescence

669 in DLD1. The plasmid vector showing Promoter 1 (e) showed an optimal mCherry readout. (h-l)
670 Lenti CMV mCherry showed an increase in mCherry fluorescence as MOI was increased from 5-
671 100. (m-q) In a similar manner, CDX2 lenti mCherry (promoter 1) was used and 50MOI was
672 chosen further for the selection of CDX2-expressing cells from the term placenta.

Figure S3

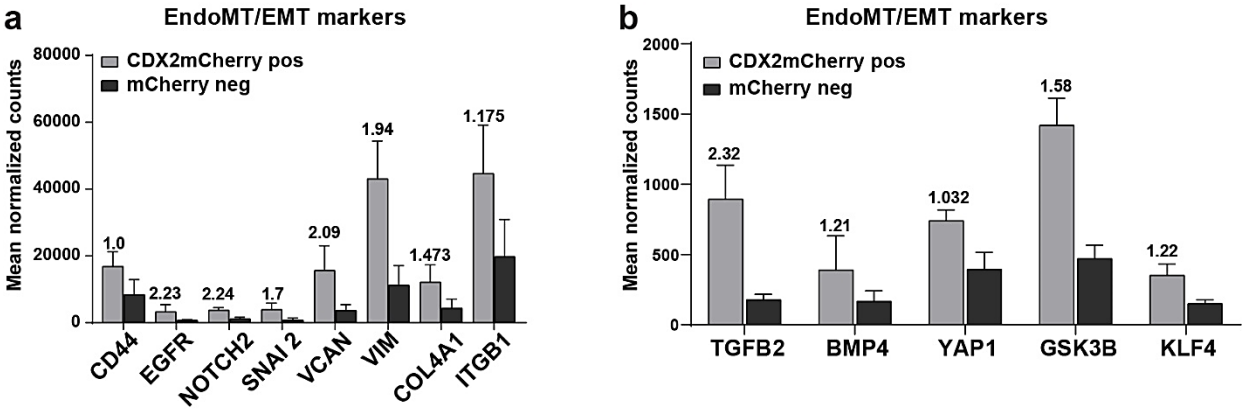

Extended Data Figure 3 : Upregulated EndoMT/EMT transcriptome in CDX2 mCherry cells

(a,b) CDX2mCherry cells show upregulated markers implicated in the endothelial-mesenchymal transition, crucial for valve formation during cardiac development. Mean normalized values are plotted in the Y-axis and Log2 fold change in comparison to mCherry negative cells are annotated above each CDX2 bar graph (n=4).

Figure S4

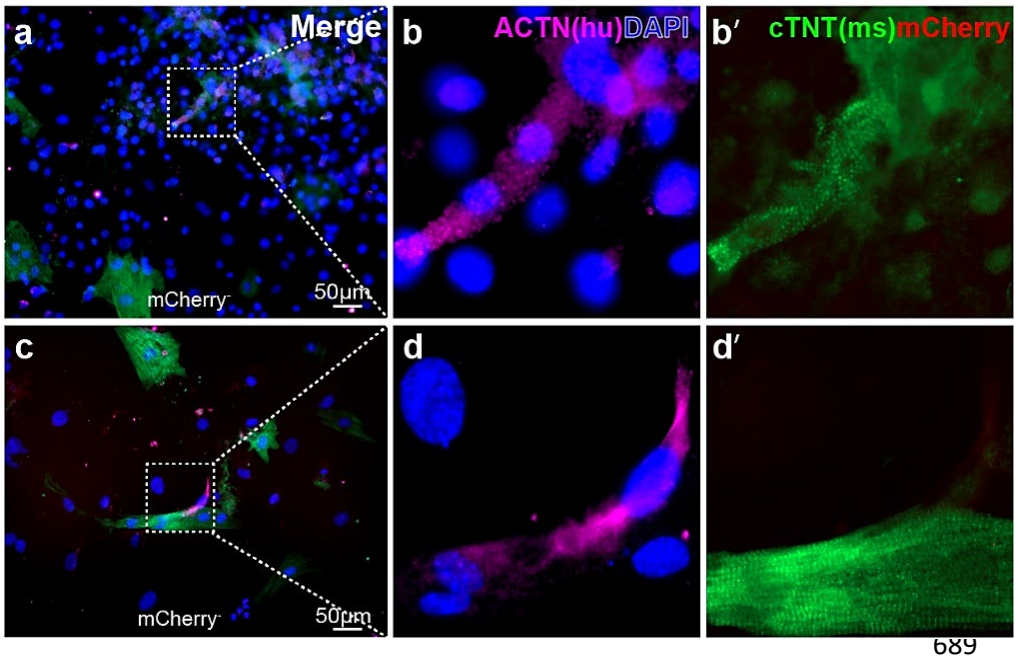

Extended Data Figure 4. Limited cardiac differentiation of mCherry negative cells on neonatal cardiomyocytes feeder (a) and (c) are representative immunofluorescence images from two different mCherry negative placenta cells on murine neonatal cardiomyocytes feeder. mCherry negative cells did not efficiently differentiate and did not show cTnT (detects both mouse and human cardiomyocytes) expression, however, weakly expressed human-specific actinin (pink-not detected in mouse myocytes). Panel (b) represent the highlighted field from overlay (a) showing human-specific actinin (pink) that only detects human myocytes whereas panel b' shows the endogenous murine cTnT (green) expression. Similarly, panel (d) represents the highlighted field from overlay image (c) representing mCherry negative cell-derived cell expressing human-specific actinin (pink), whereas cTnT (green) detects murine cardiomyocyte within the feeder.